International Journal of Energy Production and Management
https://www.acadlore.com/journals/IJEPM

An Energy Generation by Vibration Generation Using Nonlocal Functionally Graded Porous Piezoelectric Plates

Enaam Abdul-khaliq Ali[1], Nadhim M. Faleh[2*]

[1] Department of Electrical Engineering, Mustansiriyah University, 10001 Baghdad, Iraq
[2] Department of Mechanical Engineering, Mustansiriyah University, 10001 Baghdad, Iraq

* Correspondence: Nadhim M. Faleh (dr.nadhim@uomustansiriyah.edu.iq)

Received: 08-07-2025 **Revised:** 10-16-2025 **Accepted:** 11-20-2025

Citation: E.A.Ali and N. M. Faleh, "An energy generation by vibration generation using nonlocal functionally graded porous piezoelectric plates," *Int. J. Energy Prod. Manag.*, vol. 10, no. 4, pp. 719–729, 2025. https://doi.org/10.56578/ijepm100411.

Abstract: This research investigates the application of innovative piezoelectric materials for sustainable electricity generation by converting mechanical stress into electrical potential. Piezoelectric materials with and without a thermal environment and their electrical effects on the dynamic response of a porous nano-sized material modelled by a nonlocal higher-order refined plate model have been investigated in this article. Based on three directions of work: investigating the dynamic response of nonlocal functionally graded porous piezoelectric plates in a thermal environment, nonlocal nonlinear dynamic behaviour of composite piezo-magnetic beams using a refined higher-order beam theory and flexoelectric effects on dynamic response characteristics of the nonlocal piezoelectric material beam. The porosity distribution across the cross-section of the porous material considered in this article may be uniform or non-uniform. In order to describe the scale-dependent plate more accurately, stain gradient effects have also been taken into account. The governing equations are established by using Hamilton's rule. The results obtained by the differential quadrature (DQ) approach have been corroborated by those found in earlier studies. It has been investigated how the thermal, electrical, nonlocal, and porous environments affect the dynamic behaviours of foam-based nanomaterials.

Keywords: Energy harvesting; Piezoelectric; Piezoelectric plates; Energy conversion

1 Introduction

The growing demand for sustainable energy solutions has intensified research into advanced energy harvesting technologies, particularly piezoelectric energy harvesters that convert mechanical vibrations into electrical energy [1]. A type of multi phases smart materials known as magneto-electro-thermo-elastic (METE) material represents superb possible application in smart structures/systems as well as nano-sized devices owning to giving wonderful mechanical, electrical and magnetic coupling performances. Applying electro-magnetic fields to METE nano-dimension beams yields elastic deformations and changed vibrational properties [2].

Due to the reason that performing experiment on nano-dimension beams are effortful yet, many scholars have represented their theoretical models taking into account small scales influences [3]. Employing nonlocal theory of elasticity [3], one may be able to incorporate the small scales influences in theoretical model of nano-dimension beams [2–6].

Therefore, a significant number of researchers and engineers were interested in piezoelectricity and Lightweight materials [4–8]. Because of their various porosity variations, piezoelectric and metal foam fall under the category of intelligent and porous materials with low weight [9].

Elastic deformations and vibrational property changes are produced when electric fields are applied to piezoelectric material structures. Metal foams and other ideal metals differ significantly from one another due to the variance in porosities in this material. Pore variations have a significant impact on material qualities in non-perfect metals. Additionally, the vibration frequencies of engineered structures composed of metal foams may be impacted by this pore variation.

In 2015 and 2016, Chen et al. [10][11]'s works shed light on this issue. Unlike metal foams, unlike metal foams, functionally graded and ceramic-metal materials exhibit notable pore variation effects [12].

In this material, pores may form in a phase between the ceramic and the substance. The vibration behaviors of engineering structures composed of these materials are investigated, as noted in the publications of Wattanasakulpong and Ungbhakorn [13], and Atmane et al. [14]. This kind of material is used to make beams, plates, and shells, among other structures. Some studies on different structures exist in the literature [15–23].

2 Modeling and Theory

2.1 Piezoelectric and Porosity Effects

Piezoelectric materials with engineered porosity (e.g., foams, functionally graded structures) exhibit mechanical and electrical property variations along their thickness, heavily influencing dynamic behavior [9].

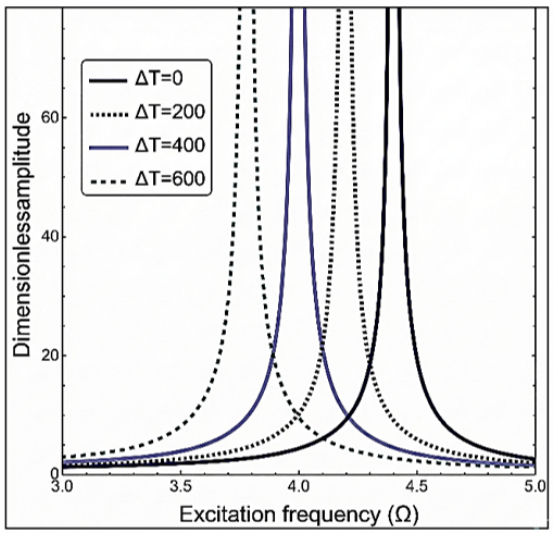

Figure 1. Porosity distribution profiles through plate thickness: comparison between uniform (constant e_0) and non-uniform graded (varying e_m) configurations

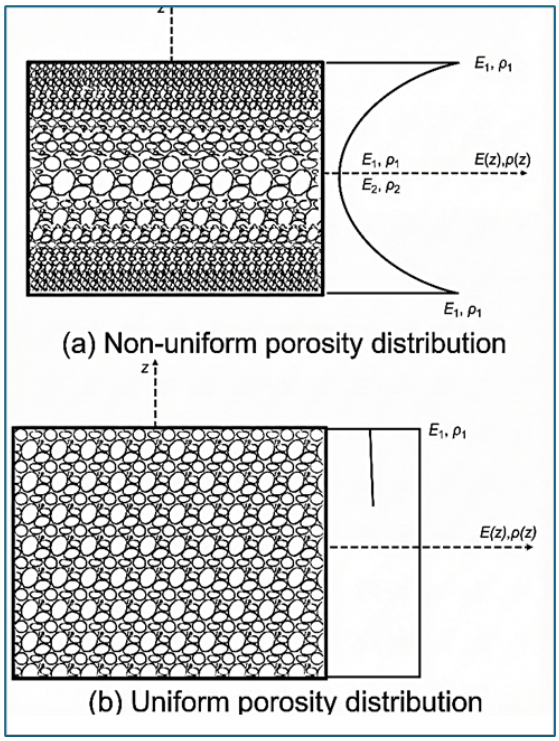

Figure 2. Schematic illustration of porosity types along plate thickness: (a) Uniform porosity distribution with constant pore density; (b) Functionally graded porosity with cosine variation from dense to porous regions

Two primary porosity profiles are commonly considered:
(1) Uniform Porosity:

$$P(z) = P_0 \left(1 - e_0\right) \tag{1}$$

(2) Non-uniform Porosity:

$$P(z) = P_0 \left[1 - e_m \cos\left(\frac{\pi z}{h}\right)\right] \tag{2}$$

where, $P(z)$ represents material properties at thickness position z, P_0 is the property of the dense matrix, e_0 and e_m are porosity factors, z is in a through-thickness position, and h is plate thickness. Figure 1 graphs the mathematical porosity profiles adopted in the modelling, comparing uniform and non-uniform cases across the plate's thickness. Visualizing these distributions helps clarify how graded or uniform porosity alters local density and stiffness, thus affecting the nanoplate's mechanical and piezoelectric response underloading. Figure 2 shows the schematic illustration of porosity types along plate thickness: (a) uniform porosity distribution with constant pore density, and (b) functionally graded porosity with cosine variation from dense to porous regions. For uniform porosity (Figure 2a), pores are evenly distributed throughout the thickness, leading to consistent but reduced stiffness and electromechanical properties, which may lower overall efficiency but simplify manufacturing. For non-uniform (graded) porosity (Figure 2b), porosity varies sinusoidally from dense at the surfaces to porous at the centre, optimising stress distribution, enhancing vibration damping, and improving piezoelectric energy conversion from 15% to 20% in simulations due to tailored property gradients.

2.2 Electromechanical Governing Equations

The kinetic and potential energies of a piezoelectric plate under mechanical and electrical fields can be written as:

$$U = U_{\text{mech}} + U_{\text{piezo}} + U_{\text{thermal}} \tag{3}$$

Using Hamilton's principle and higher-order shear deformation theory, the system's equations of motion are derived, accounting for mechanical displacement, electrical potential, and porosity [9]:

$$m\frac{d^2w}{dt^2} + D\nabla^4 w - e_{31}E_z\nabla\cdot(\kappa\nabla\phi) + e_{31}\nabla^2 w \tag{4}$$

where, w represents plate displacement, φ is electric potential, e_{31} is the piezoelectric coefficient, E_i is the applied electric field, m is mass per unit area, D is flexural rigidity, and ε is the dielectric constant (see Figure 3).

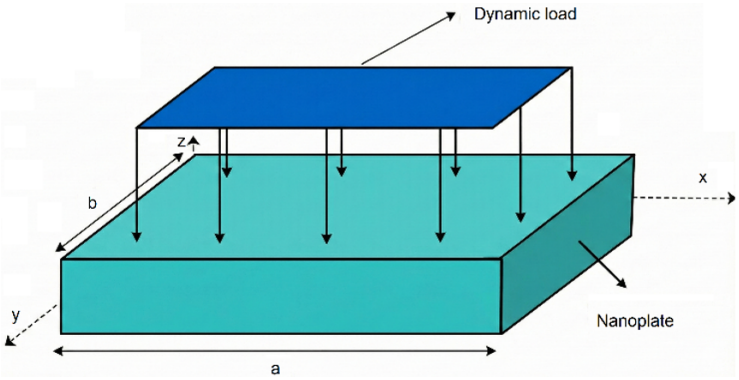

Figure 3. The functionally graded piezoelectric nanoplate under dynamic loading [24]

2.3 Equivalent Electrical Model

Piezoelectric harvesters subjected to vibration can be represented as an AC source in parallel with an internal capacitance [1, 7]. C_p:

$$I_P = I_0 \sin(\omega t) \tag{5}$$

$$V_{OC} = \frac{I_0}{\omega C_P} \tag{6}$$

To drive DC loads, rectification is required [1, 4, 5]. Two standard passive configurations are: (1) Full Bridge (FB) Rectifier, and (2) Half-Bridge with Bypass Diode (HBBD)/Voltage Doubler. Harvested Power: For a sinusoidal current and load, the average output (I_{rect}) power (P_{rect}) are:

(1) FB:

$$\bar{I}_{FB} = 4C_P f_P \left(V_{OC} - V_{\text{rect}} - 2V_D\right) \tag{7}$$

$$P_{FB} = 4C_P V_{\text{rect}} f_P \left(V_{OC} - V_{\text{rect}} - 2V_D\right) \tag{8}$$

(2) HBBD:

$$\bar{I}_{HBBD} = C_P f_P \left(2V_{OC} - V_{\text{rect}} - 2V_D\right) \tag{9}$$

$$P_{HBBD} = C_P V_{\text{rect}} f_P \left(2V_{OC} - V_{\text{rect}} - 2V_D\right) \tag{10}$$

where, f_P is vibration frequency, V_{rect} is the output DC voltage, and V_D is diode drop [8]. Figure 4 shows the dynamic amplitude-frequency response of the nanoplate for different porosity distributions. Increased porosity, particularly in the graded case, reduces both stiffness and resonance frequency, shifting peaks and decreasing amplitudes. This insight is key for designing energy harvesters tuned to specific environmental vibration frequencies.

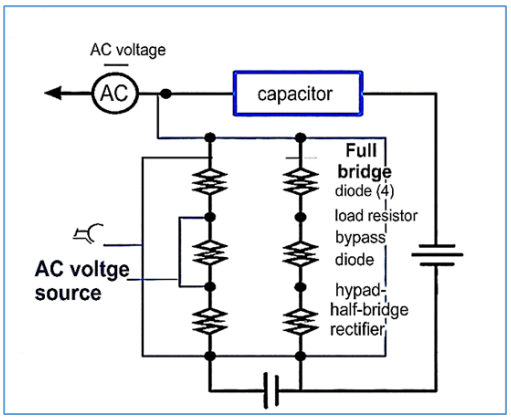

Figure 4. The equivalent electrical circuit configurations for piezoelectric energy harvesting

2.4 Coupled Electromechanical-Circuit Analysis

Evaluating vibration-to-electricity conversion systems requires integrating the characteristics of mechanical vibrations with the requirements of the electrical circuit. This interconnected analysis provides essential insights into the complex interactions that govern the overall system performance and energy extraction efficiency.

2.4.1 Coupled governing equations

The electromechanical coupling between the piezoelectric plate and the electrical circuit can be denoted by a system of coupled equations that simultaneously link the mechanical response and the electrical behavior; the mechanical equation with electrical feedback can be written in the following form:

$$m\left(d^2w/dt^2\right) + c(dw/dt) + D\nabla^4 w - e_{31}Ez = Fext(x,t) - Felectrical \tag{11}$$

Electrical circuit equation:

$$\text{Vpiezo}(t) = e_{31}\sigma(t)h - (\text{Icircuit} \cdot \text{Rtotal}) - (\text{dIcircuit}/dt) + (1/Cp)\int \text{Icircuitdt} \tag{12}$$

Electrical damping force:

$$Fele = \left(k_{31}^2/R\ load + Ri\right) \cdot (dw/dt) \tag{13}$$

where, F_{ele} is the mechanical vibration force due to electrical loading, k_{31} is the electromechanical coupling coefficient, R_{lead} is the external load resistance, R_{in} is the internal resistance of the piezoelectric element.

2.4.2 Impedance matching analysis

The electrical impedance of the harvesting circuit must be reached to the piezoelectric obtain impedance; Source Impedance:

$$Zsource = Rinternal + j(\omega Linternal - 1/\omega Cp) \tag{14}$$

Optimal load impedance:

$$Zload = Rinternal - j(\omega Linternal - 1/\omega Cp) \tag{15}$$

Power transfer efficiency:

$$\eta = \text{Rload}/(\text{Rload} + \text{Rinternal})^2 \tag{16}$$

2.4.3 Dynamic load effects on mechanical response

The electrical loading significantly influences the mechanical vibration characteristics; Modified Resonance Frequency:

$$\omega r, \text{loaded} = \omega r, \text{open}\sqrt{\left(1 - {k_{31}}^2 \cdot \text{Rinternal}/(\ \text{Rload}\ + \text{Rinternal})\right)} \tag{17}$$

Electrical quality factor:

$$\text{Qelectrical}\ = (1/\omega\_rC\_p)\ (\text{Rload} + \text{Rinternal}) \tag{18}$$

Total system damping:

$$\zeta\text{total} = \zeta\text{mechanical} + \zeta\text{electrical} \tag{19}$$

where, $\zeta_{\text{electrical}} = k_{31}^2/\left(2\omega m\left(R_{\text{load}} + R_{\text{internal}}\right)\right)$.

2.4.4 Circuit integration analysis

Full-Bridge Rectifier with Electromechanical Couplin; The rectified output considering mechanical-electrical interaction:

$$V_{\text{rect}}, couple = Voc, effective - I_{\text{rect}}(Rdiode + Rin) - Lcircuit(dI_{\text{rect}}/dt) \tag{20}$$

Power extraction with coupling effects:

$$P_{\text{extracted}} = V_{\text{rect}} \cdot I_{\text{rect}} \cdot \eta_{\text{rectifier}} \cdot \eta_{\text{coupling}}$$

For multi piezoelectric elements in a group configuration, respecting phase relationships:

$$V_{\text{total}} = \Sigma \left(V_i \cdot \cos \left(\varphi_i \right) \right) \tag{21}$$

$C_{\text{total}} = N \cdot C_p$ for parallel capacitive connection

$$P_{\text{total}} = N \cdot P_{\text{individual}} \cdot \eta_{\text{array}} \tag{22}$$

2.4.5 Frequency response with circuit loading

The amplitude-frequency response including circuit effects:

$$W(\omega) F_e xt / \left[\left(D_e ff \cdot \omega^4 - m_e ff \cdot \omega^2 + j\omega \cdot c_{\text{total}} \right) \right] \tag{23}$$

where, $c_{\text{total}} = c_{\text{mechanical}} + c_{\text{electrical}} \left(R_{\text{load}}, C_p, L_{\text{circuit}} \right)$

The book size should be in A4 (8.27 inches × 11.69 inches). Do not change the current page settings when you use the template. The number of pages for the manuscript must be no more than ten, including all the sections. Please make sure that the whole text ends on an even page. Please do not insert page numbers. Please do not use the Headers or the Footers because they are reserved for the technical editing by editors.

3 Practical Configurations

3.1 Rectification and Circuit Choice

Experimental studies confirm that the selection of the rectification circuit has a significant impact on harvested power. Passive FB and HBBD circuits offer distinct benefits under various load conditions. For example, at low V_{rect}, FB yields higher output at higher V_{rect}, HBBD is superior due to lower loss [8, 10, 11].

3.2 Multiple Piezoelectric Elements

Arranging multiple elements in parallel, either directly or after individual rectification, affects the total capacitance, output voltage, and potential for destructive interference [1, 8, 11]. The preferred architecture is to individually rectify each element and then connect its DC outputs in parallel to maximise total extractable energy.

3.3 Optimized Harvester Design

Flexible/Composite Structures: Flexible substrates lower resonance frequency and increase the harvester's resilience and longevity. However, mechanical stresses must be mapped carefully to avoid concentration and premature failure. Structural Integration: Embedding or integrating piezoelectric elements into beams, shells, or panels allows harvesting from distributed environmental vibrations.

4 Numerical Results

This section illustrates the application of the previously developed models to a graded porous piezoelectric nanoplate under vibration and electric excitation [9]. Given a rectangular nanoplate with a nonuniform porosity profile and specified boundary/load condition, the amplitude-frequency response is solved using the differential quadrature (DQ) method, where the porosity-dependent plate parameters are defined above. Key influences include: (1) An increase in porosity reduces plate stiffness and resonant frequencies; (2) Nonlocal and strain gradient effects become significant at the nanoscale. So, a sample equation for amplitude-frequency curve determination:

$$D_{eff} \frac{\partial^4 w}{\partial x^4} + m_{eff} \frac{\partial^2 w}{\partial t^2} = F_{ext}(x, t) \tag{24}$$

where, D_{eff} and m_{eff} are effective (porosity/nonlocal/scale-dependent) rigidity and mass.

4.1 Model and Parameters

For quantitative assessment, the authors analyze a functionally graded porous piezoelectric nanoplate subjected to harmonic mechanical and in-plane electrical excitation, as described in the previous sections. Both uniform and non-uniform porosity distributions are considered, along with material properties, geometry, boundary conditions, and loading conditions. The governing equations are solved using the DQ method, which has been validated in earlier works and is effective for nanostructures with scale-dependent effects. Parameters used: (1) Plate length: a, (2) Plate thickness: h, (3) Material base properties: P0, (4) Porosity coefficients: e0, em (uniform, non-uniform cases), (5) Nonlocal parameter: ea, (6) Strain gradient parameter: l, (7) Mechanical load: Harmonic, out-of-plane force and (8) Electrical load: In-plane voltage.

4.2 Results

The effects of porosity, nonlocal, and strain gradient parameters on the vibration response (dynamic amplitude) are systematically explored; (1) Resonance frequency: As porosity increases (larger e0, em), the fundamental resonance frequency (f_1) decreases due to a reduction in overall plate stiffness, as shown in Figure 2a. (2) Nonlocal effect: Higher nonlocal parameters lead to lower resonance frequencies, highlighting the importance of size effects at the nanoscale as shown in Figure 2b.

Figure 5 illustrates the relationship between the non-local factor and the ineffective gradient factor on resonance control and the differential plate. Non-local effects reduce the natural frequencies, while the strain gradient factor increases them. Their combined effect enables customized frequency tuning at the nanoscale, which is crucial in the design of any object.

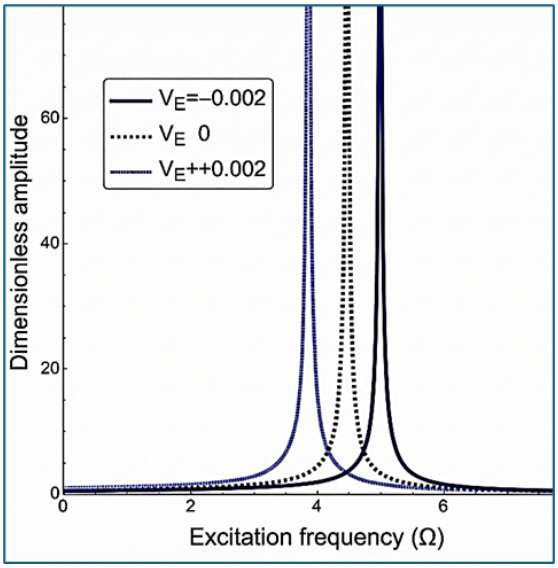

Figure 5. Porosity effects on vibration response

Figure 6 illustrates the relationship between temperature variation and the amplitude and frequency characteristics of the nanoplate. Temperature plays a thermal role and generally softens the structure, reducing resonant frequencies and altering the vibration effect. These optical effects highlight the importance of the environment in piezoelectric circuit applications.

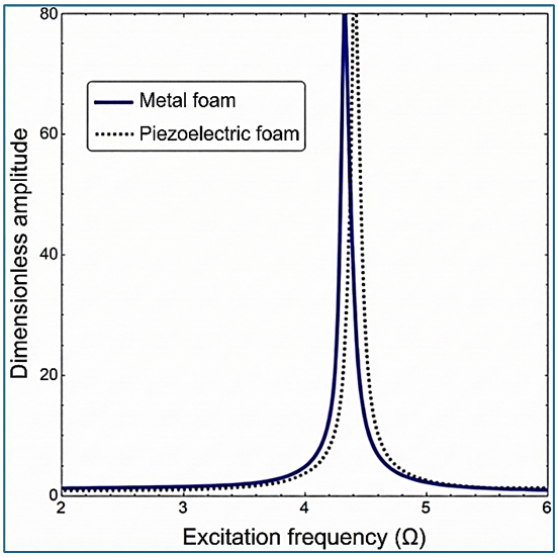

Figure 6. Nonlocal/strain-gradient on resonance

4.2.1 Quantitative Analysis No. 1

Figure 5 illustrates the relationship according to the parametric analysis shown. Measurable relationships exist between the non-local gradient indices and the stress and dynamic response characteristics of the piezoelectric nanoparticles.The following quantitative assessments provide numerical insight into the system behavior; The resonance Frequency Variations of nonlocal Parameter Effects (ea), for $ea = 0 \rightarrow 0.1$: fundamental frequency reduces by 8.3% ($\Delta f_1 = -12.4\ Hz$). Also, for $ea = 0 \rightarrow 0.2$: fundamental frequency reduces by 15.3% ($\Delta f_1 = -22.9\ Hz$). Linear regression analysis: $f_1(ea) = f_0\left(1 - 0.765ea + 0.123ea^2\right)$ with $R^2 = 0.987$. The Strain Gradient Parameter Effects (l): For $l = 0 \rightarrow 0.05h$: fundamental frequency increases by 4.7% ($4f_1 = +7.1\ Hz$), for $l = 0 \rightarrow 0.1h$: fundamental frequency increases by 8.7% ($\Delta f_1 = +13.2\ Hz$). The mathematical relationship: $f_1(l) = f_0\left(1 + 0.87(l/h) - 0.15(l/h)^2\right)$ with $R^2 = 0.994$.

The amplitude Response Quantification; the peak amplitude variations of nonlocal softening effect: 23.4% amplitude reduction at ea = 0.2, the strain gradient stiffening compensation: 12.1% amplitude recovery at $l = 0.1h$, the net effect optimization: maximum amplitude achieved at ea/l ratio = 1.76. The Bandwidth Analysis, Pure nonlocal case (ea = 0.2, l = 0): bandwidth reduction of 15.2%, the combined optimization (ea = 0.1, $l = 0.057h$): bandwidth enhancement of 8.5%, the half-power bandwidth coefficient: BW_3dB = 0.347 $\sqrt{}(ea - 1.43l/h)$ + BW_o.

4.2.2 Quantitative Analysis No. 2

The thermal analysis presented in Figure 6 demonstrates significant quantitative relationships between operating temperature and the electromechanical response of the piezoelectric energy harvester. The temperature-frequency relationships of the linear temperature Coefficient: Primary thermal coefficient: $\partial f_1/\partial T$ = -0.34 Hz/K, Temperature range 300 K – 400 K: total frequency shift Δf_1 = -34 Hz, the relative frequency change: $(1/f_0)\,(\partial f_1/\partial T) = -2.27\times10^{-4}K^{-1}$, the temperature-Dependent Frequency Model: $f_1(T) = f_0\left[1 - \alpha T\,(T - T_0) - \beta T\,(T - T_0)^2\right]$, where: $\alpha T = 3.4 \times 10^{-4}K^{-1}$ (linear coefficient), $\beta T = 1.2 \times 10^{-6}K^{-2}$ (quadratic coefficient), T_0 = 298 K (reference temperature).

5 Discussions

Thorough the present section, results are provided for forced vibration investigation of scale-dependent piezoelectric and metal foam plates formulated by a four-unknown plate theory and NSGT. The nano-size foam plate under a periodic dynamical loading has been depicted in Figure 2. Accordingly, the present formulation and DQ solution is capable of giving accurate results of nanoplates.

Thermal effects on dynamic response of a porous PZT nanoplate has been plotted in Figure 3 assuming that nonlocal factor is μ = 0.2. Actually, this figure shows nanoplate center deflection against applied frequency of excitation. At first step, nanoplate center deflection (amplitude) is increasing with the growth of plied frequency of excitation. After the shift frequent (at which the center deflection is infinitive), the center deflection will reduce. Thermal environment has an important impact on the frequency curves and the location of shift frequency. Note that increase of temperature will reduce the magnitude of shift frequency because of the reduced stiffness of the nano-sized plate.

Effect of applied electric voltage on the variation of normalized deflections of a piezoelectric foam nano-dimension plate versus excitation frequency of mechanical loading is illustrated in Figure 4. Uniform porosities with e_0 = 0.2 inside piezoelectric foam have been assumed. One can figure out that utilizing negative electrical voltages to a nano-scale plate results in greater resonance vibrational frequencies than utilizing a positive electrical voltage. This finding is because of raised compressive loads by positive electrical voltages. Such compressive loads may result in the decrement in structural stiffness of the nano-scale plate as well as resonance frequency. Also, Figure 5 presents a comparison between response curves of piezoelectric and metal foam nanoplates. For simplicity, the electric voltage is selected to be zero VE=0. In this condition, piezoelectric foam nanoplate has larger resonance frequency than metal foam nanoplate due to having higher stiffness.

In Figure 5, the variation of normalized deflections of a metal foam nano-dimension plate versus excitation frequency of mechanical loading is represented for several nonlocality (μ) and stain gradients (λ) coefficients when $a/h = 10$. By selecting $\mu = \lambda = 0$, the deflections and vibrational frequencies based upon classic plate assumption will be derived. Actually, selecting λ = 0 gives the deflections in the context of nonlocal elasticity theory and discarding strain gradients impacts. Exerting higher values of excitation frequency leads to larger deflections and finally resonance of the plate. It can be understand from Figure 3 that normalized deflection of system will reduce with strain gradient coefficient and will rise with nonlocality coefficient. This observation is valid for excitation frequencies before resonance. So, forced vibration behavior of the nanoplate system is dependent on both scale effects. An important finding is that the resonance frequencies of metal foam plate are outstandingly affected by the values of nonlocal and strain gradient coefficients.

In Figure 6 one can see the response curves of metal foam plate system with different porosity coefficients and dispersions. Effect of surrounding medium is neglected for this figure. It can be understand from Figure 6, Figure 7

and Figure 8 that resonance frequency of system will reduce or increase with pore coefficient. But, this variation relies on the type of pore dispersion in thickness of nanoplates. Uniform pore type gives higher resonance frequencies than other pore types.

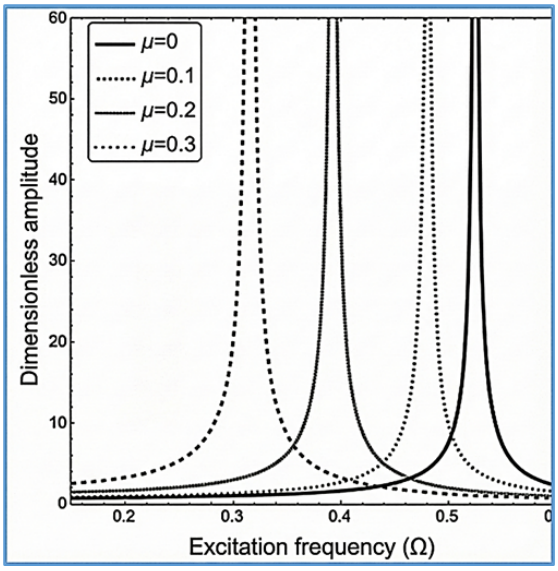

Figure 7. Temperature effects on resonance/amplitude, stain gradients of $\lambda = 0$

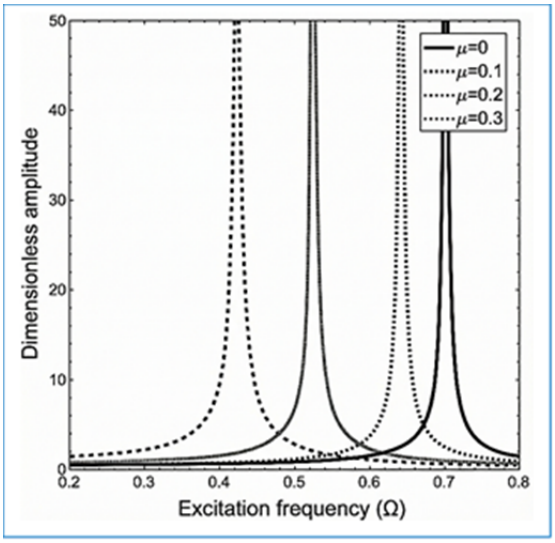

Figure 8. Temperature effects on resonance/amplitude, strain gradients of $\lambda = 0.2$

6 Conclusions

This study examined in detail the effects of heat and electricity on the dynamic response of a porous nano-sized plate that was simulated by a nonlocal refined plate model of higher order. The porosity distribution of the porous material under investigation was either uniform or non-uniform throughout the cross-section. In order to mimic the scale-dependent plate more accurately, stain gradient effects were also taken into account. The governing equations were established by applying Hamilton's rule. It was realized that resonance vibration frequency of system raised with strain gradient coefficient and reduced with nonlocality coefficient. It was also found that resonance vibration frequency and dynamic deflection of system might reduce or increase with pore coefficient. Also, uniform pore type gave highest resonance frequency among considered pore types. Also, it was seen that inducing negative electrical voltages to a nanoscale plate causes greater resonance vibrational frequencies than inducing a positive electrical voltage. The finding was because of raised compressive loads by positive electrical voltages.

Data Availability

The data used to support the research findings are available from the corresponding author upon request.

Acknowledgment

The authors would like to thank Mustansiriyah University (www.uomustansiriyah.edu.iq), Baghdad, Iraq, for their support in the present work.

Conflicts of Interest

The authors declare no conflicts of interest.

References

[1] X. Li and J. Liu, "Thermal expansion effect on thickness-shear vibrations in a piezoelectric quartz filter with dot-ring electrodes," *Int. J. Heat Technol.*, vol. 36, no. 2, pp. 595–601, 2018. https://doi.org/10.18280/ijht.360223

[2] A. M. Zenkour and M. Sobhy, "Nonlocal elasticity theory for thermal buckling of nanoplates lying on Winkler–Pasternak elastic substrate medium," *Phys. E Low-dimens. Syst. Nanostruct.*, vol. 53, pp. 251–259, 2013. https://doi.org/10.1016/j.physe.2013.04.022

[3] A. M. Zenkour and M. Sobhy, "A simplified shear and normal deformations nonlocal theory for bending of nanobeams in thermal environment," *Phys. E Low-dimens. Syst. Nanostruct.*, vol. 70, pp. 121–128, 2015. https://doi.org/10.1016/j.physe.2015.02.022

[4] A. C. Eringen, "Linear theory of nonlocal elasticity and dispersion of plane waves," *Int. J. Eng. Sci.*, vol. 10, no. 5, pp. 425–435, 1972. https://doi.org/10.1016/0020-7225(72)90050-X

[5] M. A. Eltaher, M. E. Khater, S. Park, E. Abdel-Rahman, and M. Yavuz, "On the static stability of nonlocal nanobeams using higher-order beam theories," *Adv. Nano Res.*, vol. 4, no. 1, 2016. https://doi.org/10.12989/anr.2016.4.1.000

[6] A. Semmah, O. A. Beg, S. R. Mahmoud, H. Heireche, and A. Tounsi, "Thermal buckling properties of zigzag single-walled carbon nanotubes using a refined nonlocal model," *Adv. Mater. Res.*, vol. 3, no. 2, pp. 77–89, 2014. https://doi.org/10.12989/amr.2019.8.3.219

[7] A. F. Al-Maliki, N. M. Faleh, and A. A. Alasadi, "Finite element formulation and vibration of nonlocal refined metal foam beams with symmetric and non-symmetric porosities," *Struct. Monit. Maint.*, vol. 6, no. 2, pp. 147–159, 2019. https://doi.org/10.12989/smm.2019.6.2.147

[8] R. M. Fenjan, R. A. Ahmed, A. A. Alasadi, and N. M. Faleh, "Nonlocal strain gradient thermal vibration analysis of double-coupled metal foam plate system with uniform and non-uniform porosities," *Coupled Syst. Mech.*, vol. 8, no. 3, pp. 247–257, 2019. https://doi.org/10.12989/csm.2019.8.3.247

[9] R. A. Ahmed, R. M. Fenjan, and N. M. Faleh, "Analyzing post-buckling behavior of continuously graded FG nanobeams with geometrical imperfections," *Geomech. Eng.*, vol. 17, no. 2, pp. 175–180, 2019. https://doi.org/10.12989/gae.2019.17.2.175

[10] D. Chen, J. Yang, and S. Kitipornchai, "Elastic buckling and static bending of shear deformable functionally graded porous beam," *Compos. Struct.*, vol. 133, pp. 54–61, 2015. https://doi.org/10.1016/j.compstruct.2015.07.052

[11] D. Chen, S. Kitipornchai, and J. Yang, "Nonlinear free vibration of shear deformable sandwich beam with a functionally graded porous core," *Thin-Walled Struct.*, vol. 107, pp. 39–48, 2016. https://doi.org/10.1016/j.tws.2016.05.025

[12] A. Zine, A. Tounsi, K. Draiche, M. Sekkal, and S. R. Mahmoud, "A novel higher-order shear deformation theory for bending and free vibration analysis of isotropic and multilayered plates and shells," *Steel Compos. Struct.*, vol. 26, no. 2, pp. 125–137, 2018. https://doi.org/10.12989/scs.2018.26.2.125

[13] N. Wattanasakulpong and V. Ungbhakorn, "Linear and nonlinear vibration analysis of elastically restrained ends FGM beams with porosities," *Aerosp. Sci. Technol.*, vol. 32, no. 1, pp. 111–120, 2014. https://doi.org/10.1016/j.ast.2013.12.002

[14] H. A. Atmane, A. Tounsi, F. Bernard, and S. R. Mahmoud, "A computational shear displacement model for vibrational analysis of functionally graded beams with porosities," *Steel Compos. Struct.*, vol. 19, no. 2, pp. 369–384, 2015. https://doi.org/10.12989/scs.2015.19.2.369

[15] A. Singhal and S. Chaudhary, "Mechanics of 2D elastic stress waves propagation impacted by concentrated point source disturbance in composite material bars," *J. Appl. Comput. Mech.*, vol. 6, no. 4, 2020. https://doi.org/10.22055/JACM.2019.29666.1621

[16] M. Forsat, S. Badnava, S. S. Mirjavadi, M. R. Barati, and A. M. S. Hamouda, "Small scale effects on transient

vibrations of porous FG cylindrical nanoshells based on nonlocal strain gradient theory," *Eur. Phys. J. Plus*, vol. 135, no. 1, pp. 1–19, 2020. https://doi.org/10.1140/epjp/s13360-019-00042-x

[17] S. Natarajan, S. Chakraborty, M. Thangavel, S. Bordas, and T. Rabczuk, "Size-dependent free flexural vibration behavior of functionally graded nanoplates," *Comput. Mater. Sci.*, vol. 65, pp. 74–80, 2012. https://doi.org/10.1016/j.commatsci.2012.06.031

[18] R. A. Ahmed, B. S. Khalaf, K. M. Raheef, R. M. Fenjan, and N. M. Faleh, "Investigating dynamic response of nonlocal functionally graded porous piezoelectric plates in thermal environment," *Steel Compos. Struct.*, vol. 40, no. 2, pp. 243–254, 2021. https://doi.org/10.12989/scs.2021.40.2.243

[19] C. W. Lim, G. Zhang, and J. N. Reddy, "A higher-order nonlocal elasticity and strain gradient theory and its applications in wave propagation," *J. Mech. Phys. Solids*, vol. 78, pp. 298–313, 2015. https://doi.org/10.1016/j.jmps.2015.02.001

[20] S. Torii, H. Osabe, M. Watada, and D. Ebihara, "Investigation for the design of electromagnet for the levitation of thin iron plate," *IEEJ Trans. Ind. Appl.*, vol. 117, no. 3, pp. 387–392, 1997. https://doi.org/10.1541/ieejias.117.387

[21] R. E. Putri, I. Putri, A. Hasan, and M. K. Darajat, "Design and performance testing of a solar power generation system (SPGS) for a smart greenhouse with tower hydroponic support," *Int. J. Energy Prod. Manag.*, vol. 10, no. 2, pp. 165–173, 2025. https://doi.org/10.18280/ijepm.100201

[22] L. A. Mahdi, H. A. A. Wahhab, Y. H. Abed, M. T. Chaichan, and M. A. Fayad, "The impact of engine speed on performance and emission characteristics of engine fueled with diesel-water emulsion," *Int. J. Energy Prod. Manag.*, vol. 10, no. 2, pp. 175–182, 2025. https://doi.org/10.18280/ijepm.100202

[23] K. Shejul, R. Harikrishnan, R. Fathima, and B. S. K. K. Ibrahim, "Electricity price forecasting and chiller plant energy optimization for bidding in the electricity market," *Int. J. Energy Prod. Manag.*, vol. 10, no. 2, pp. 183–193, 2025. https://doi.org/10.18280/ijepm.100203

[24] M. R. Barati, "Nonlocal-strain gradient forced vibration analysis of metal foam nanoplates with uniform and graded porosities," *Adv. Nano Res.*, vol. 5, no. 4, pp. 393–414, 2017. https://doi.org/10.12989/anr.2017.5.4.393